Advances in Nano Research, *Vol. 5 No. 4 (2017) 373-392*
DOI: https://doi.org/10.12989/anr.2017.5.4.373

Nelumbo nucifera extracts mediated synthesis of silver nanoparticles for the potential applications in medicine and environmental remediation

N. Supraja [1], B. Avinash [2] and T.N.V.K.V. Prasad [*1]

[1] *Nanotechnology laboratory, Institute of Frontier Technology, Regional Agricultural Research Station, Acharya N.G. Ranga Agricultural University, Tirupathi – 517502, A.P., India*
[2] *Department of Veterinary Parasitology, College of Veterinary Sciences, Sri Venkateswara Veterinary University, Tirupati – 517502, A.P., India*

(*Received February 22, 2017, Revised June 20, 2017, Accepted July 20, 2017*)

Abstract. Silver nanoparticles (AgNPs) were successfully synthesized through a simple green route using the *Nelumbo nucifera* leaf, stem and flower extracts. These nanoparticles showed characteristic UV-Vis absorption peaks between 410-450 nm which arises due to the plasmon resonance of silver nanoparticles. The Fourier transform infrared spectroscopy (FT-IR) confirmed the presence of amides and which acted as the stabilizing agent. X-ray diffraction spectrum of the nanoparticles confirmed the Face centered cubic (FCC) structure of the formed AgNPs. Dynamic light scattering technique was used to measure hydrodynamic diameter (68.6 nm to 88.1 nm) and zeta potential (-55.4 mV, -57.9 mV and 98.9 mV) of prepared AgNPs. The scanning electron micrographs of dislodged nanoparticles in aqueous solution showed the production of reasonably monodispersed silver nanoparticles (1-100 nm). The antimicrobial activity of prepared AgNPs was evaluated against fungi, Gram-positive and Gram-negative bacteria using disc diffusion method. Anti-corrosion studies were carried out using coupon method (mild steel and iron) and dye degradation studies were carried out by assessing photo-catalytic activity of *Nelumbo nucifera* extracts mediated AgNPs.

Keywords: *Nelumbo nucifera*; silver nanoparticles; antimicrobial activity; corrosion; photo-catalytic activity

1. Introduction

The advent of the nanoscale materials has given new insights into the problem tackling in the fields of medicine, pharmaceuticals, and electronics. Recent years have shown remarkable progress in research and development of metallic nanoparticles that takes advantage of their unique optical, magnetic, electronic, catalytic and other physicochemical properties in a wide range of practical and potential applications such as energy, environment, biomedical and chemical engineering (Hirsch *et al*. 2005). Among the nanomaterials, noble metal nanoparticles have many important applications in medicine and pharmacy. For instance, silver nanoparticles can be used in medicine to reduce infection in burn treatment, to prevent bacteria colonization on dental materials,

*Corresponding author, Ph.D., E-mail: tnvkvprasad@gmail.com

http://www.techno-press.org/?journal=anr&subpage=5 ISSN: 2287-237X (Print), 2287-2388 (Online)

stainless steel materials, to eliminate microorganisms on textile fabrics, and for water treatment (Panacek *et al*. 2006, Bo *et al*. 2009, Tomsic *et al*. 2008).

Although, many chemical methods are available to reduce silver nitrate into silver nanoparticles, use of high-end chemicals and toxicity of the residual chemical restricts the production and application of silver nanoparticles (Alarcon *et al*. 2012, Panacek *et al*. 2009, Prucek *et al*. 2011, Shanmugam *et al*. 2014). As an alternate, researchers are revealing their interest in the synthesis of metallic nanoparticles through green technology (Rastogi and Arunachalam 2011, Vijayakumar *et al*. 2011, Yilmaz *et al*. 2011, Guidelli *et al*. 2011, Kouvaris *et al*. 2012). Many researchers have reported the biosynthesis of metal nanoparticles by plant leaf extracts and their potential applications (Salem *et al*. 2014, Abdel-Aziz *et al*. 2014, Sulaiman *et al*. 2013, Prabhu *et al*. 2013). *Nelumbo nucifera* (Lotus), an aquatic plant with medicinal values, is seen in India and China. This species can be multiplied either by sexual (seeds) or asexual (rhizomes) reproduction. *N. nucifera* is reported to have anti diarrheal and antimicrobial properties. A number of researchers have reported on synthesis of metallic nanoparticles including silver (Prabha *et al*. 2014), gold (Sreekanth *et al*. 2014), copper oxide (Padil and Cernik 2013), zinc nanoparticles using different plant materials.

Nelumbo nucifera is a monogeneric plant belongs to the family Nelumbonaceae, commonly known as sacred Indian lotus, *Nelumbo nucifera* is a perennial ornamental water plant grown in Asian countries for its edible rhizomes and seeds. The plant has some unique features like; the ability to regulate the temperature of its flowers within a narrow range (Yoon 1996), seeds with long viability periods (Shen-Miller *et al*. 1995) and in addition its leaves show the lotus effect, the self-cleaning property. Various lotus plant parts have been used as herbal medicines for treatment of many diseases including cancer, depression, diarrhea, heart problems, hypertension and insomnia (Shen *et al*. 2002, Duke *et al*. 2001). Lotus produces a number of important secondary metabolites, like alkaloids, flavonoids, steroids, triterpenoids, glycosides and polyphenols (Mukherjee *et al*. 2009). It is an important folklore medicinal plant, which would prevent cancer development (Yoon *et al*. 2013). It has also shown its efficacy in antibacterial, antiviral and antiplatelet activity (Brindha and Arthi 2010).

Therefore, in the present investigation, pink *N. nucifera* leaf, stem and flower extracts were used to prepare silver nanoparticles. The antimicrobial activity of *N. nucifera* silver nanoparticles was evaluated (*in-vitro*) against pathogenic fungi and bacteria using disc diffusion method. Anti-corrosion efficacy was evaluated using coupons method and dye-degradation studies were carried out through photo-catalytic activity of *N. nucifera* silver nanoparticles.

2. Materials and methods

2.1 Collection of microbes (*Bacteria and fungi*)

The microbes (Bacteria and fungi) samples were collected from Nanotechnology laboratory, Regional Agricultural Research Station, Tirupathi, Chittoor District, Andhra Pradesh, India. These samples were stored in an ice box and transported to the laboratory for microbiological characterization. Through serial dilution pour plate technique, fungal sp. was isolated using potato dextrose agar (PDA) medium, and Gram negative and Gram-positive bacteria were isolated from nutrient agar medium. Further, it is maintained in potato dextrose agar slants (fungi) and nutrient agar slants (bacteria) for onward analysis. The test organisms include *Aspergillus niger*,

Aspergillus flavus, *Rhizopus oligosporus*, *Sclerotium rolfsii*, *E.coli*, *Bacillus subtilis*, *Pseudomonos fluorescence*, and *Staphylococcus aureus*.

2.2 Collection of plant material

Healthy *Nelumbo nucifera* plant was collected from Tirumala hills, Andhra Pradesh state, India. From the selected plant, leaves, stem and flower was collected by scrapping using neat and clean knife during the month of April 2014, and collected materials were carefully washed and dried at 45°C to constant weight. The dried plant materials were powdered, passed through a BSS no. 85-mesh sieve, and stored in air-tight container.

2.3 Preparation of Nelumbo nucifera plant extracts (Leaf, Stem and Flowers)

The collected *Nelumbo nucifera* plant was allowed to shade dried for 72 h and was ground to get fine powder. Then, 10 g of powder (leaf, stem and flower) was mixed with 100 mL of distilled water (DW unit, Bhanu industries, Banglore) and boiled for 40 min. After that, the extract was filtered by using Whatman No. 1 filter paper and collected the filtrate in plastic bottle and stored at 4°C for further experimentation.

2.4 Biosynthesis of silver nanoparticles

Aqueous solution (90 mL) of 1.0×10^{-3} M silver nitrate was mixed with a 10 mL of 10 % aqueous solution of *Nelumbo nucifera* plant extracts (leaf, stem and flower) extract. The samples were then centrifuged using REMI K70 at 4000 rpm (2146 g) for 15min to get clear supernatant. The initial concentration of the AgNPs was measured using inductively coupled plasma optical emission spectrophotometer (ICP-OES) and was found to be 170±1.4ppm. Then, the sample was diluted to different concentrations of 170, 100, and 30 ppm and they were used to investigate the concentration-dependent antimicrobial effect of AgNPs. These silver nanoparticles were characterized by using the techniques such as X-ray diffractometry (XRD), Fourier transform infrared spectrophotometry (FTIR), UV–Vis spectrophotometry, dynamic light scattering (particle size), zeta potential and scanning electron microscopy (SEM).

2.5 Measurement of concentration of AgNPs using inductively coupled plasma optical emission spectrophotometer (ICP-OES)

The concentrations of the AgNPs were measured using ICP-OES (Prodigy XP, Leeman Labs, USA). The samples were prepared with ten times dilution after centrifugation at 4000 rpm for 15 min. Then, 20 ml of aliquot was loaded to the racks of automatic sampler, and the concentration of AgNPs was estimated thrice.

2.6 Characterization of silver nanoparticles

2.6.1 UV–Visible spectrum for synthesized nanoparticles

The UV–Vis spectrum of this solution was recorded in spectra 50 ANALYTIKJENA Spectrophotometer, which was operated in the wavelength range of 400–800 nm. The localized surface plasmon resonance (LSPR) of the silver nanoparticles was recorded and which is the

characteristic UV–Vis absorbance of silver nanoparticles.

2.6.2 FT-IR analysis for synthesized nanoparticles

The FT-IR spectrum was taken in the mid IR region of 400–4000 cm^{-1}. The spectrum was recorded using attenuated total reflectance technique. The sample was directly placed in the KBr crystal and the spectrum was recorded in the transmittance mode.

2.6.3 X-ray diffraction analysis for synthesized nanoparticles

The crystalline structure of the nanoparticles was determined using the XRD technique. The XRD pattern was recorded using computer controlled XRD-system, JEOL, and Model: JPX-8030 with Cu Kα radiation (Ni filtered = 13,418 A°) at the range of 40 kV, 20 A. The 'peak search' and 'search match' program built in software (syn master 7935) was used for the identification of XRD peak.

2.6.4 Particle size and zeta potential analyzer for synthesized nanoparticles

The aqueous suspension of the synthesized nanoparticles was filtered through a 0.22 lm syringe driven filter unit, and the hydro dynamic diameter (HDD) of the distributed nanoparticles was measured by the principle of dynamic light scattering (DLS) using Nanopartica (HORIBA, SZ-100) compact scattering spectrometer.

2.6.5 Scanning electron microscopy (SEM)—surface morphology studies

The surface morphological studies of the AgNPs samples were carried out with scanning electron microscope (SEM) (Hitachi's SU6600) at magnification ranging from 10 to 600,0000 operated at an accelerating voltage of 30 kV.

2.7 Antimicrobial activity of plant biosynthesized silver nanoparticles

The antimicrobial activity of *Nelumbo nucifera* extracts silver nanoparticles was examined on the basis of colony formation by *in-vitro* Petri dish assays (disc diffusion). Each fungal and bacterial isolates was cultured on growth media that induced prolific conidia and bacterial production. The fungus isolates were grown on potato dextrose agar medium, and bacterial isolates were grown on nutrient agar medium. Conidia were collected from cultures that were incubated at 37°C for 10 days (fungi), and bacterial cultures were collected from cultures that were incubated at 37°C for 2 days for (bacteria) and diluted with sterile, deionized water to a concentration of 10^6 spores ml^{-1}. Aliquots of the conidial suspension and bacterial suspension were mixed with serial concentrations of silver preparations to a final volume of 1ml and were also mixed with sterile, deionized water as control. A 10µl subsample of the conidia and A. scholaris silver mixture stock was taken at 30 ± 0.8, 100 ± 1.1 and 170 ± 1.4 ppm after silver treatments and diluted 100-fold with the deionized water. A 10 μl aliquot of the diluted spore suspension was spread on PDA (Becton, Dickson and Company, Sparks, MD) medium. Three PDA plates for fungi and three NA plates for bacteria per each combination of exposure silver concentration were tested. The filter paper disc dipped in different ppm and inserted on mediums (PDA), and then, the plates were incubated at 37°C for 2–4 days for fungi and bacteria, respectively. The average number of colonies from silver-treated spore suspensions (fungi) and (bacteria) was compared with the number on the water control (percent colony formation). The zone size was determined by measuring the diameter of the zone in mm (Aneja 2003).

2.8 Corrosion studies

Weight loss measurements provide a general idea on the extent of corrosion rates. Mild steel and iron coupons of 1×1 size with a hole on the top were used for weight loss experiments. The coupons were Machine polished to mirror finish, degreased with trichloroethylene, and rinsed with de-ionized Water coupons pre-weighted were immersed in experimental samples (*Nelumbo nucifera* leaf, stem and flower extracts mediated synthesized AgNPs, System-I; AgNPs with bacterial cultures, System-II AgNPs without bacterial cultures). These systems were kept stirred for 16days. The weight loss of the metal obtained in milligrams was converted to corrosion rate in Milli meter per year (mm/year).

2.9 Photo-catalytic degradation of dye

Typically 10 mg of methylene blue dye was added to 1000 mL of double distilled water used as stock solution. About 10 mg of biosynthesized silver nanoparticles (*Nelumbo nucifera* leaf, stem and flower) was added to 100 mL of methylene blue dye solution. A control was also maintained without addition of silver nanoparticles. Before exposing to irradiation, the reaction suspension was well mixed by being magnetically stirred for 30 min to clearly make the equilibrium of the working solution. Afterwards, the dispersion was put under the sunlight and monitored from morning to evening sunset. At specific time intervals, aliquots of 2-3 mL suspension were filtered and used to evaluate the photo-catalytic degradation of dye. The absorbance spectrum of the supernatant was subsequently measured using UV-Vis spectrophotometer at the different wavelength. The initial concentration of dye was measured by UV–Vis spectroscopy the absorbance value shown at 290 nm.

2.10 Statistical analysis

All of the data from three independent replicate trials were subjected to analysis using Statistical package for the Social Sciences (SPSS) version 16.0. The data are reported as the mean ± SD.

3. Results and discussion

3.1 UV–Vis (UV-Visible spectroscopy) analysis

Once the *Nelumbo nucifera* plant extracts (Fig. 1) (10 ml) was treated with 90 ml of silver nitrate solution, the yellow color of the solution changed to dark brown color in < 5 min. The brown color was primarily due to the surface plasmon resonance of the formed silver nanoparticles. The UV–vis absorption spectrum of the synthesized silver nanoparticles is presented in (Figs. 2(a), (b) and (c)). UV–Vis spectroscopy was employed to record the localized surface plasmon resonance of the silver nanoparticles. The maximum absorbance peak for *Nelumbo nucifera* leaf extract is observed at 410 nm, *Nelumbo nucifera* stem extract is observed at 450 nm and *Nelumbo nucifera* flower extract is observed at 420 nm. The overall observations suggest that the bio-reduction of (silver ions) $Ag^{(+)}$ to $Ag^{(0)}$ was confirmed by UV–Vis spectroscopy.

3.2 FT-IR (Fourier transformance infrared spectrophotometry) analysis

The interface between bio-organic functional groups and metal nanoparticles were illustrated

Fig. 1 Photograph showing *Nelumbo nucifera* plant (leaf, stem and flower)

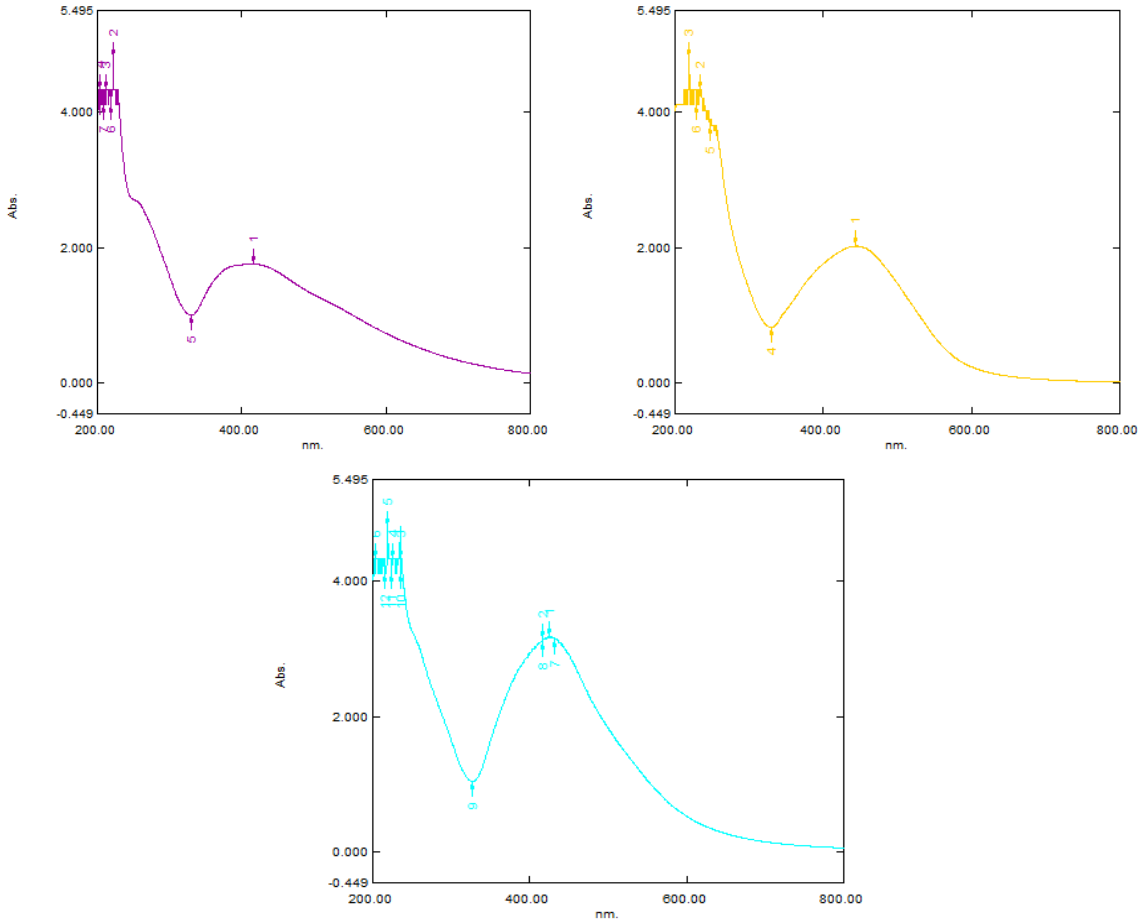

Fig. 2 UV–visible spectroscopic micrograph showing the localized surface plasmon resonance (LSPR) of Ag nanoparticles synthesized using *Nelumbo nucifera* (a) leaf; (b) stem; and (c) flower extracts

by FT-IR spectrum. FT-IR spectrum of the biosynthesized silver nanoparticles using *Nelumbo nucifera* leaf extract (Fig. 3(a)) shows the absorption peaks at 3788.80, 3348.33, 2906.01, 2886.17, 1745.22, 1640.12, 1533.80, 1481.93, 1378.49, 1164.64, 1046.99 and 889.77 cm^{-1}. The peak

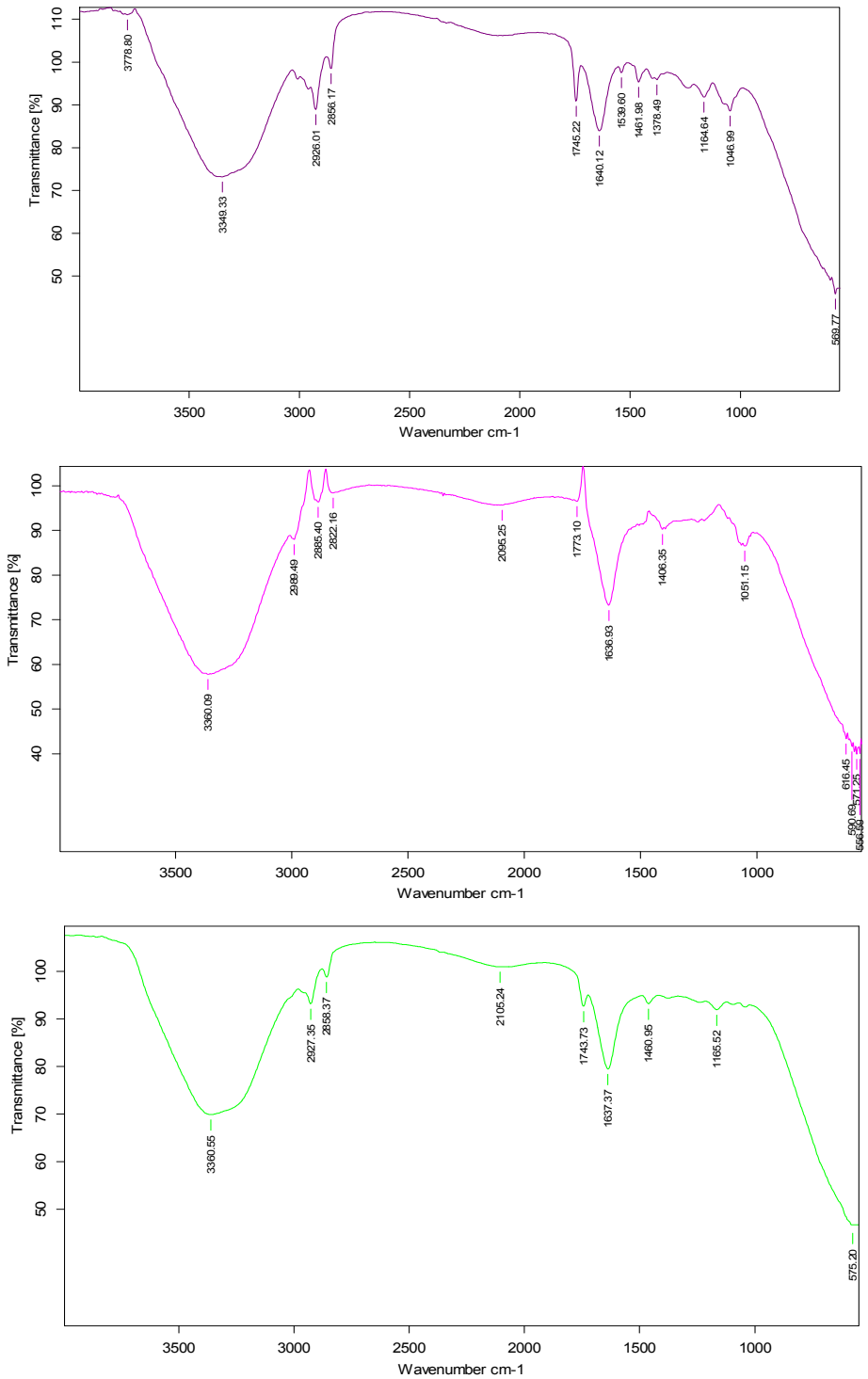

Fig. 3 FT-IR spectroscopic micrograph representing the functional groups responsible for the reduction and stabilization of Ag nanoparticles synthesized using *Nelumbo nucifera* (a) leaf; (b) stem; and (c) flower extracts

present at 3788.80 cm^{-1} reveals the presence of O-H stretching vibration of amides, 3348.33 cm^{-1} reveals the presence of C-H stretching vibration of alkynes, 2906.01, 2886.17 cm^{-1} reveals the presence of C-H stretching vibration of alkanes, 1745.22 cm^{-1} reveals the presence of C = O stretching vibration of aldehydes, 1640.12 cm^{-1} reveals the presence of –C = C- stretching vibration of alkenes, 1533.80, 1481.93 cm^{-1} reveals the presence of N-O stretching vibration of nitro compounds, 1378.49 cm^{-1} reveals the presence of C-H rock stretching vibration of alkanes, 1164.64 cm^{-1} reveals the presence of C-H wag stretching vibration of alkyl halides, 1046.99 cm^{-1} reveals the presence of C-N stretching vibration of aliphatic amines and 889.77 cm^{-1} reveals the presence of C-Cl stretching vibration of alkyl halides.

FT-IR spectrum of the biosynthesized silver nanoparticles using *Nelumbo nucifera* stem extract (Fig. 3(b)) shows the absorption peaks at 3380.09, 2989.43, 2886.40, 2822.16, 2086.25, 1773.10, 1636.93, 1406.36, 1061.15, 616.46, 580.88, 571.25 and 566.29 cm^{-1}. The peak present at 3380.09 cm^{-1} reveals the presence of C-H stretching vibration of alkynes, 2989.43 and 2886.40 cm^{-1} reveals the presence of C-H stretching vibration of alkanes, 2822.16 cm^{-1} reveals the presence of C-H stretching vibration of aldehydes, 2086.25 cm^{-1} reveals the presence of –C = C- stretching vibration of alkynes, 1773.10 cm^{-1} reveals the presence of C = O stretching vibration of carboxylic acids, 1636.93 cm^{-1} reveals the presence of –C = C- stretching vibration of alkenes, 1406.36cm^{-1} reveals the presence of C-C stretching vibration of aromatics, 1061.15 cm^{-1} reveals the presence of C-N stretching vibration of aliphatic amines, 580.88, 571.25 and 566.29 cm^{-1} reveals the presence of C-Br stretching vibration of alkyl halides.

FT-IR spectrum of the biosynthesized silver nanoparticles using *Nelumbo nucifera* flower extract (Fig. 3(c)) shows the absorption peaks at 3380.55, 2927.35, 2888.37, 2106.24, 1743.73, 1637.37, 1480.96, 1186.62 and 575.20 cm^{-1}. The peak present at 3380.55 cm^{-1} reveals the presence of C-H stretching vibration of alkynes, 2927.35 and 2888.37 cm^{-1} reveals the presence of C-H stretching vibration of alkanes, 2106.24 cm^{-1} reveals the presence of –C = C- stretching vibration of alkynes. 1743.73 cm^{-1} reveals the presence of C = O stretching vibration of carboxylic acids, 1637.37 cm^{-1} reveals the presence of N-H bend stretching vibration of primary amines, 1480.96 cm^{-1} reveals the presence of C-H bend stretching vibration of alkanes, 1186.62 cm^{-1} reveals the presence of C-H wag stretching vibration of alkyl halides and 575.20 cm^{-1} reveals the presence of C-Br stretching vibration of alkyl halides. Primary amine groups of N–H bending and carbonyl stretching vibrations of protein, respectively, indicating the involvement of proteins in reduction and stabilization of silver ions. The nanoparticles are bound to the functional organic groups (carboxyl and amine) from the *Nelumbo nucifera* plant extracts, and these functional groups may act as template, reducing and capping agents of silver nanoparticles.

3.3 XRD (X-Ray diffraction) analysis

X-ray diffraction pattern of *Nelumbo nucifera* plant extracts (Leaf, stem and flower) mediated synthesis of silver nanoparticles shows the peaks correspond to the Bragg's reflections of (111), (200), (220), (311) and (222) planes, which confirms the face-centered cubic (FCC) crystalline structure of silver (Fig. 4a, b and c). XRD analysis showed intense peaks at 2θ values of 38.08°, 53.62°, 65.67°, 76.67° and 83.54° corresponding to Bragg's reflection based on the fcc structure of silver nanoparticles. The intensity data were collected over a 2θ range of 10°–90°. A definite line broadening of the XRD peaks indicates that the prepared material consists of particles in nanoscale range. This clearly indicates that the silver nanoparticles formed by the reduction of Ag+ ions by the *Nelumbo nucifera* plant extracts are crystalline in nature. The relatively higher intensity of (111)

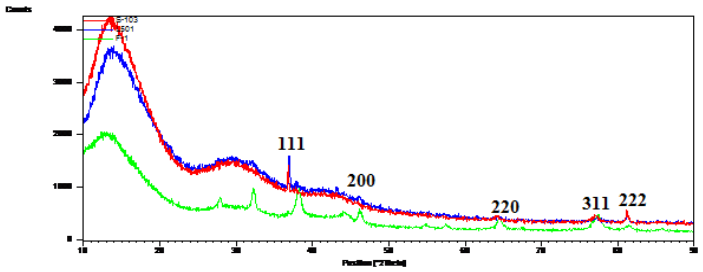

Fig. 4 XRD micrograph with the recorded Bragg's reflections corresponds to the FCC crystal structure of the silver nanoparticles synthesized using *Nelumbo nucifera* (a) leaf; (b) stem; and (c) flower extracts

and (222) plane in FCC crystal structure supports the enhanced antimicrobial activity of the prepared AgNPs. The crystalline size was calculated from the width of the peaks present in the XRD pattern, assuming that they are free from non-uniform strains, using the Debye–Scherrer formula

$$D = 0.94\lambda / \beta \cos\theta$$

Where D is the average crystalline domain size perpendicular to the reflecting planes, λ (1.5406 $\times 10^{-10}$) is the X-ray wavelength used, b is the full width at half maximum (FWHM) and h is the diffraction angle (Prasad *et al*. 2011). The calculated crystalline size of the AgNPs was 50 nm.

3.4 DLS (Dynamic light scattering) analysis

Particle size and zeta potential values were measured using Nanopartica SZ-100 (HORIBA). The zeta potential spectra for the *Nelumbo nucifera* leaf extract nanoparticles were recorded zeta

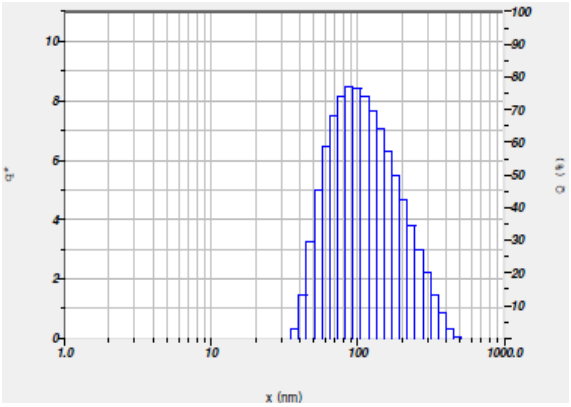

Calculation Results

Peak No.	S.P.Area Ratio	Mean	S. D.	Mode
1	1.00	127.6 nm	72.6 nm	87.7 nm
2	---	--- nm	--- nm	--- nm
3	---	--- nm	--- nm	--- nm
Total	1.00	127.6 nm	72.6 nm	87.7 nm

(a)

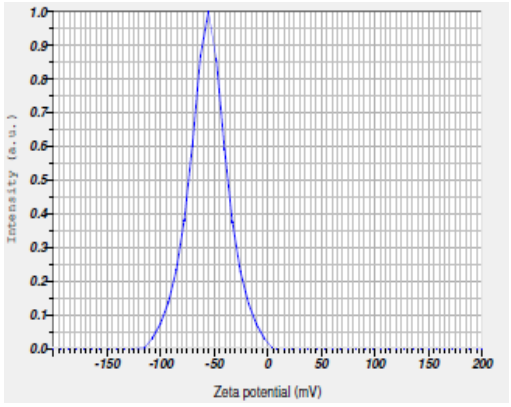

Calculation Results

Peak No.	Zeta Potential	Electrophoretic Mobility
1	-55.4 mV	-0.000430 cm2/Vs
2	--- mV	--- cm2/Vs
3	--- mV	--- cm2/Vs

Zeta Potential (Mean) : -55.4 mV
Electrophoretic Mobility mean : -0.000430 cm²/Vs

(b)

Fig. 5 Histogram (size distribution) of silver nanoparticles (dynamic light scattering) and zeta potential (-55.4 mV) of silver nanoparticles synthesized using *Nelumbo nucifera* leaf extract

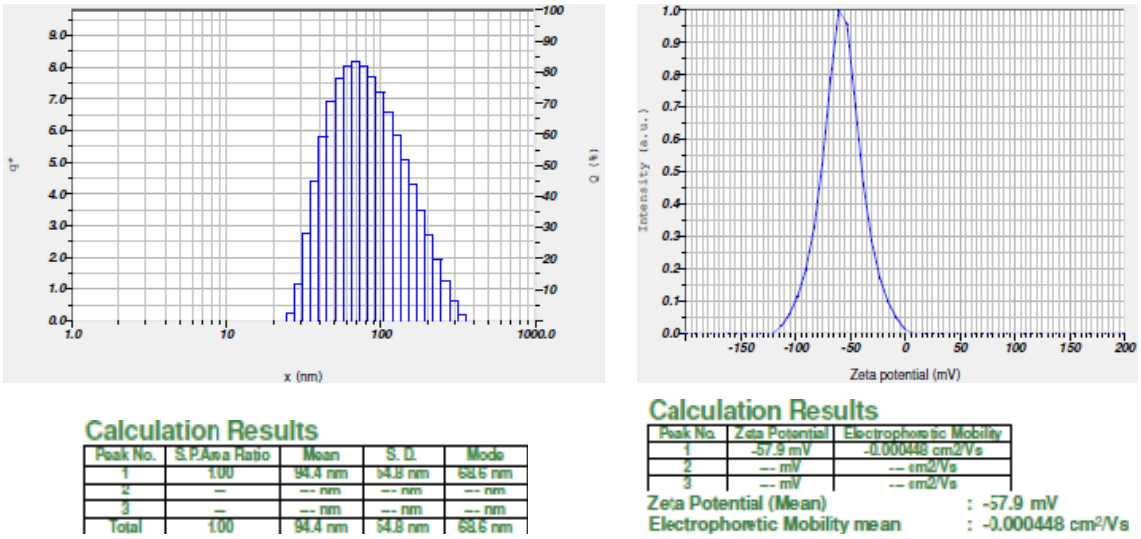

(a) (b)

Fig. 6 Histogram (size distribution) of silver nanoparticles (dynamic light scattering) and zeta potential (-57.9 mV) of silver nanoparticles synthesized using *Nelumbo nucifera* stem extract

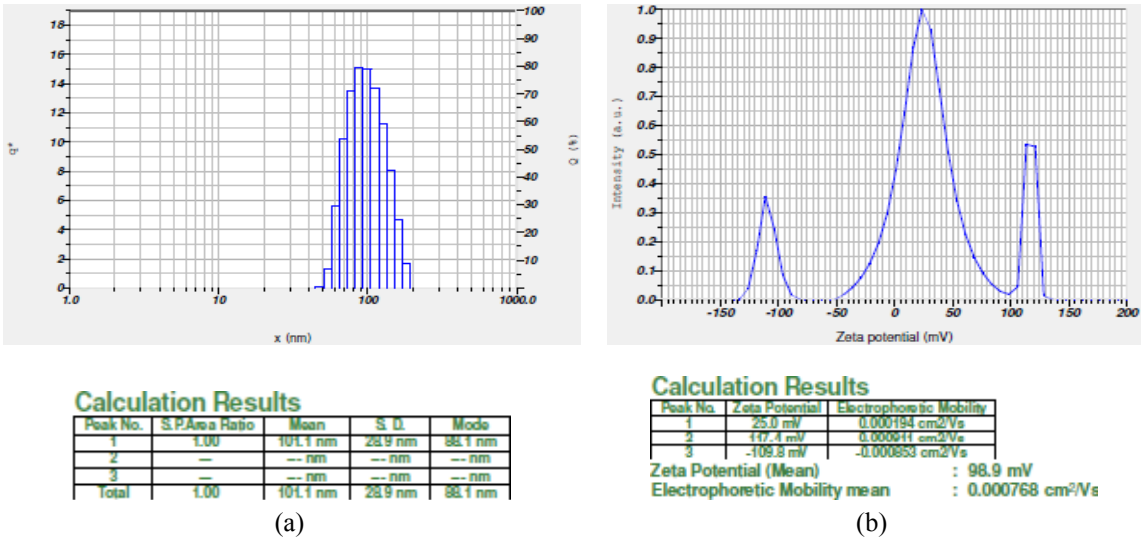

(a) (b)

Fig. 7 Histogram (size distribution) of silver nanoparticles (dynamic light scattering) and zeta potential (98.9 mV) of silver nanoparticles synthesized using *Nelumbo nucifera* flower extract

potential verses intensity spectra with zeta potential (mV) on *x*-axis and intensity (a.u) on y-axis particle size of 87.7 nm and zeta potential of -55.4 mV were recorded (Figs. 5(a) and (b)), *Nelumbo nucifera* stem extract nanoparticles particle size of 68.6nm and zeta potential of -57.9 mV were recorded (Figs. 6(a) and (b)) and *Nelumbo nucifera* flower extract nanoparticles particle size of 88.1 nm and zeta potential of 98.9mV were recorded (Figs. 7(a) and (b)). If the hydrosols

have a large negative or positive zeta potential then they will tend to repel with each other and there will be no tendency of the particles to agglomerate. For the silver nanoparticles synthesized from *Nelumbo nucifera* plant extracts, least particle size and high zeta potential values were recorded. The stability of the nanoparticles in colloidal dispersions was explained by zeta potential indicating the degree of repulsion between the adjacent and similarly charged particles in the dispersion media. Here the zeta potential value of the silver nanoparticles indicated good stability with high potential (Sri Sindhura *et al*. 2013).

3.5 SEM (Scanning Electron Microscopy) analysis

The morphology of *Nelumbo nucifera* extracts samples shows the crystalline nature by formation of repetitive layers the size of the crystals was noticed to be approximately 1–20 μm (Leaf 20 μm, Stem 5 μm and Flower 1 μm). The higher magnification SEM image clearly shows silver nanoparticles were seen as crystals. These are generally either aggregates of triangular, spherical, elongated and cubic or flower shaped crystals (Fig. 8).

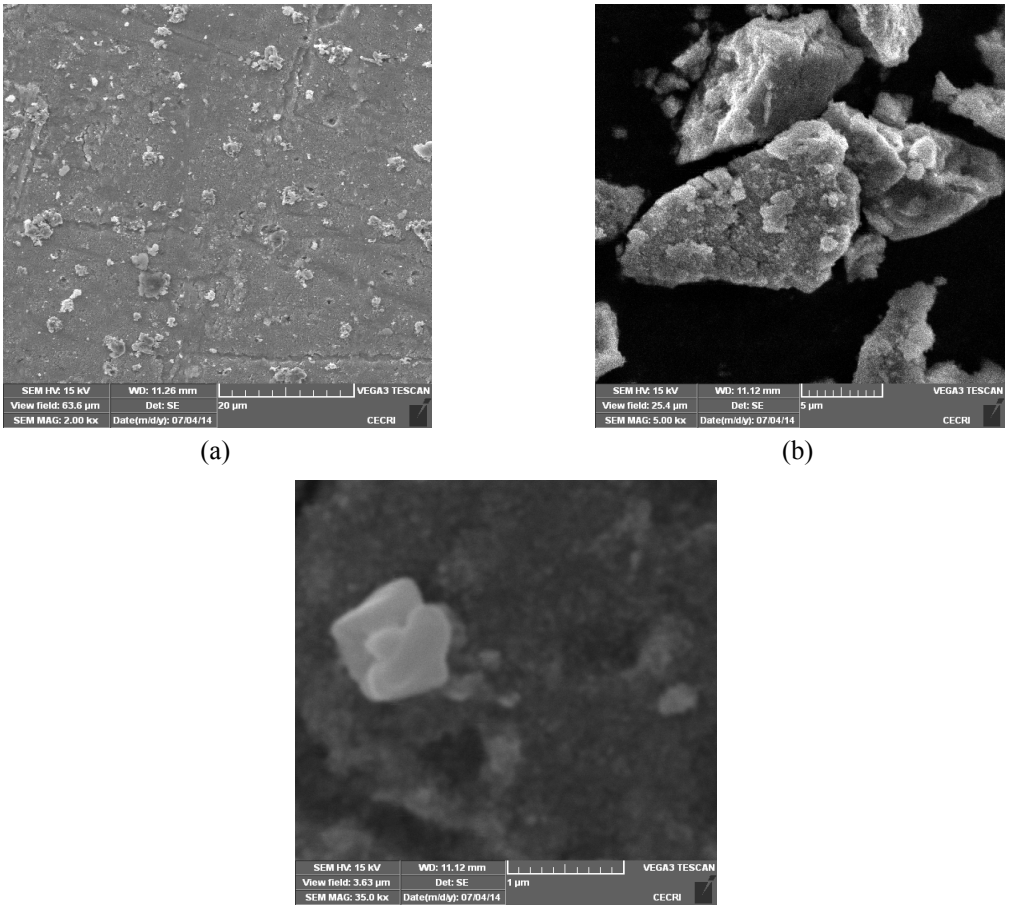

(a) (b)

(c)

Fig. 8 (a) Leaf; (b) stem; and (c) flower: SEM micrograph (bar size 1-50 μm) of *Nelumbo nucifera* silver nanoparticles showing spherical, triangular and flower shaped particles

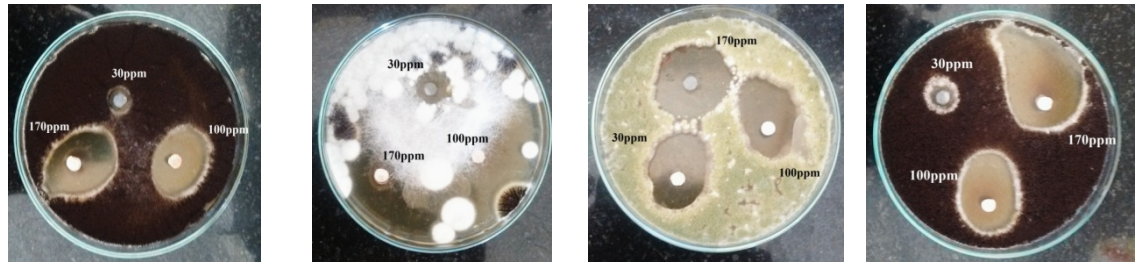

(a)

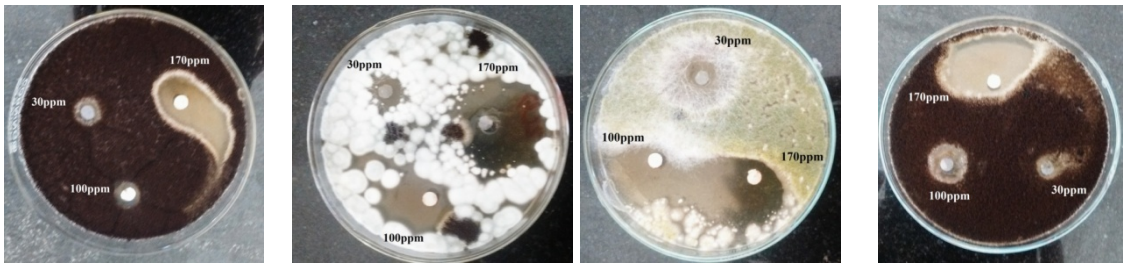

(b)

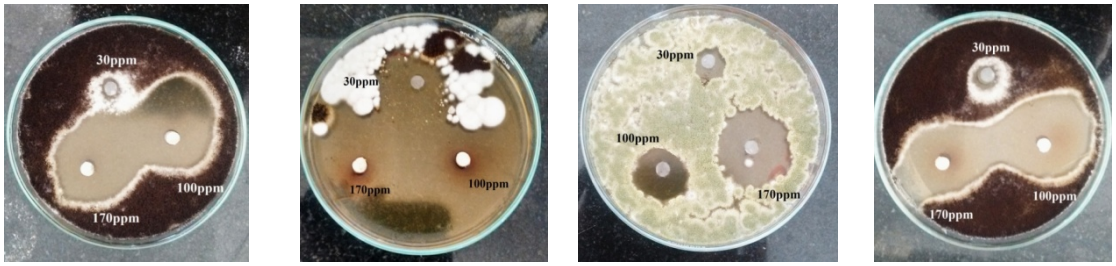

(c)

Aspergillus niger *Sclerotium rolfsii* *Rhizopus oligosporus* *Aspergillus flavus*

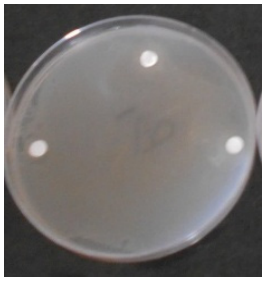

Control

Plate 1 Antifungal activity of different concentrations (30,100,170 ppm) of *Nelumbo nucifera* (a) leaf; (b) stem; and (c) flower extract-mediated AgNPs

3.6 Antimicrobial efficacy of Nelumbo nucifera biosynthesized silver nanoparticles

Silver nanoparticles obtained from *Nelumbo nucifera* plant extracts (leaf, stem and flower) have shown very strong inhibitory action against fungal sp, Gram-positive and Gram-negative

bacteria (Plates 1 and 2). Three concentrations of AgNPs (170, 100, 30 ppm) were prepared and were applied against an array of fungal species *viz*, *Aspergillus niger*, *Rhizopus oligosporus*, *Aspergillus flavus*, *Sclerotium rolfsii* and bacterial species *viz*., *E. Coli*, *Bacillus subtilis*, *Pseudo-*

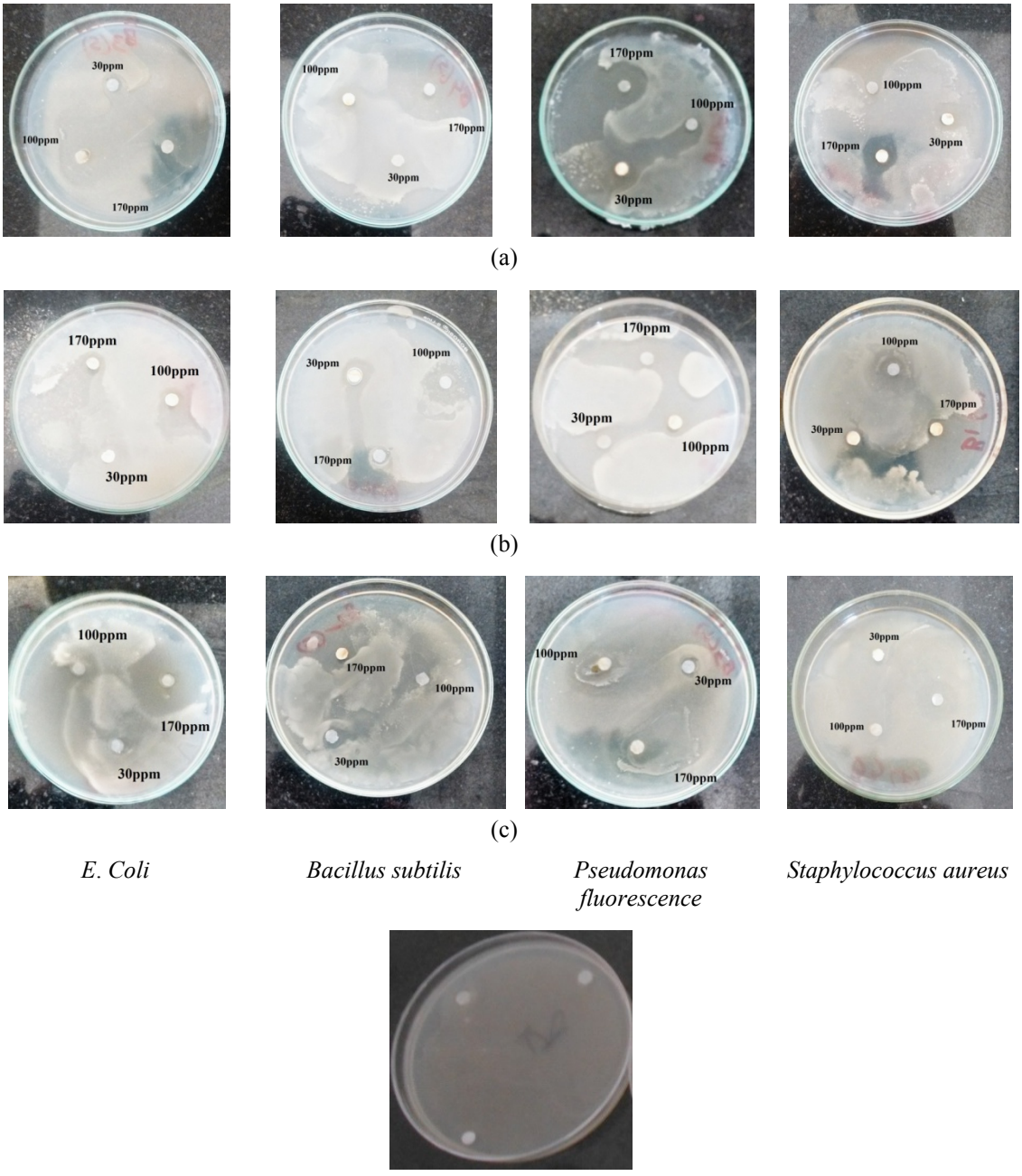

Plate 2 Antibacterial activity of different concentrations (30,100,170 ppm) of *Nelumbo nucifera* (a) leaf; (b) stem; and (c) flower; extract-mediated AgNPs

monas fluorescence and *Staphylococcus aureus*. The higher concentration (170 ppm) of flower mediated synthesized AgNPs showed significant antimicrobial effect (Tables 1 and 2) compared with other concentrations (100, 30 ppm) seen in leaf and stem. The inhibitory action of the microbes may be attributed to the loss of replication ability of DNA upon treatment with the silver ion, besides the fact that expression of ribosomal sub-unit proteins as well as some other cellular proteins and enzymes essential to ATP production becomes inactivated (Kouvaris *et al*. 2012). The higher antimicrobial activity of smaller-sized nanoparticles than their bulk counterparts could be due to the large surface area to volume ratio and the surface activity (Sivakumar *et al*. 2012). Further, the fact is that nanoparticles are more abrasive in nature than bulk $AgNO_3$, thus contributing to the greater mechanical damage to the cell membrane resulting in enhanced fungal effect. It is believed that microorganisms carry a negative charge while metal oxides carry a positive charge. This creates an ''electromagnetic'' attraction between the microbe and treated surface. But to understand the mechanisms of action of these agents, more detailed chemical structure elucidation of the bioactive components followed by therapeutic investigations and toxicological assessment are required.

Table 1 *In-vitro* antifungal studies against fungal pathogens using *Nelumbo nucifera* Extract (Leaf-L, Stem-S and Flower-F) mediated silver nanoparticles

S.No	Fungi	*Nelumbo nucifera* silver nanoparticles Zone of inhibition (mm)								
		Leaf extract			Stem extract			Flower extract		
		170 ppm	100 ppm	30 ppm	170 ppm	100 ppm	30 ppm	170 ppm	100 ppm	30 ppm
1	*Aspergillus niger*	2.5±0.8	2.2±0.6	0.6±0.2	2.0±0.2	1.4±0.2	0.5±0.01	3.6±0.5	3.2±1.2	1.3±0.5
2	*Sclerotium rolfsii*	2.7±0.6	2.3±0.7	0.9±0.4	2.6±0.4	1.3±0.5	0.6±0.08	4.5±1.2	4.4±0.8	4.2±0.3
3	*Rhizopus oligosporus*	2.9±0.4	2.7±0.3	2.3±0.5	2.7±0.6	2.6±0.4	0.9±0.04	3.8±0.9	3.4±1.2	2.3±0.4
4	*Aspergillus flavus*	3.0±0.5	2.7±0.6	1.2±0.1	2.3±0.4	1.3±0.2	0.6±0.05	4.1±1.3	3.8±0.9	2.4±0.5

Table 2 *In-vitro* antibacterial studies against bacterial pathogens using *Nelumbo nucifera* Extract (Leaf, Stem and Flower) mediated silver nanoparticles

S.No	Fungi	*Nelumbo nucifera* silver nanoparticles Zone of inhibition (mm)								
		Leaf extract			Stem extract			Flower extract		
		170 ppm	100 ppm	30 ppm	170 ppm	100 ppm	30 ppm	170 ppm	100 ppm	30 ppm
1	*E. Coli*	3.5±0.8	2.9±0.4	0.9±0.08	3.0±0.4	2.8±0.5	0.8±0.4	4.6±0.4	4.2±0.7	2.3±0.2
2	*Bacillus subtilis*	3.9±1.2	2.7±0.8	0.7±0.03	2.9±0.5	2.7±0.2	1.3±0.8	3.8±0.5	3.0±0.6	2.2±0.4
3	*Pseudomonas fluorescence*	4.0±0.9	3.2±0.2	2.9±0.04	2.9±0.4	2.7±0.4	2.4±0.5	3.3±0.7	3.0±0.5	1.0±0.6
4	*Staphylococcus aureus*	3.3±1.4	2.8±0.6	1.1±0.08	3.0±0.8	2.3±0.2	1.6±0.3	2.9±0.3	2.3±0.4	1.4±0.2

3.7 Weight loss (*Corrosion coupon study*)

Weight loss of mild steel and iron coupons in the presence and absence of bacteria is presented in (Table 3). In the system presence of bacteria and AgNPs, the weight loss for lotus leaf AgNPs in iron coupon 33.0 mg and corrosion rate was 1.907 mm/y, mild steel coupon 23.8 mg and corrosion rate was 1.375 mm/y. The weight loss for lotus stem AgNPs in iron coupon 37.5 mg and corrosion rate was 2.167 mm/y, mild steel coupon 12.6 mg and corrosion rate was 0.728 mm/y. The weight loss for lotus flower AgNPs in iron coupon 08.6 mg and corrosion rate was 0.497 mm/y, mild steel coupon 0.24 mg and corrosion rate was 0.138 mm/y. Control system in the absence of bacteria the

Table 3 Weight loss and corrosion study for mild steel and iron coupons in presence of *Nelumbo nucifera* extracts (Leaf, Stem and Flower) mediated synthesized silver nanoparticles

System	Weight loss (mg)						Corrosion rate (mm/y)					
	Mild steel coupon (L)	Iron coupon (L)	Mild steel coupon (S)	Iron coupon (S)	Mild steel coupon (F)	Iron coupon (F)	Mild steel coupon (L)	Iron coupon (L)	Mild steel coupon (S)	Iron coupon (S)	Mild steel coupon (F)	Iron coupon (F)
Experiment	23.8 (Bac + NPs)	33.0 (Bac + NPs)	12.6 (Bac + NPs)	37.5 (Bac + NPs)	0.24 (Bac + NPs)	08.6 (Bac + NPs)	1.375 (Bac + NPs)	1.907 (Bac + NPs)	0.728 (Bac + NPs)	2.167 (Bac + NPs)	0.138 (Bac + NPs)	0.497 (Bac + NPs)
Control	18.9 (AgNPs)	20.5 (AgNPs)	10.2 (AgNPs)	24.4 (AgNPs)	0.19 (AgNPs)	0.39 (AgNPs)	1.092 (AgNPs)	1.185 (AgNPs)	0.589 (AgNPs)	0.141 (AgNPs)	0.001 (AgNPs)	0.002 (AgNPs)

(a) (b) (c)

In absence of bacteria (only AgNPs)

(d) (e) (f)

In presence of bacteria + AgNPs

Fig. 9 (a) Leaf; (b) stem; and (c) flower; shows Weight loss studies of *Nelumbo nucifera* silver nanoparticles (coupons- mild steel and iron)

weight loss for lotus leaf AgNPs in iron coupon 20.5 mg and corrosion rate was 1.185 mm/y, mild steel coupon 18.9 mg and corrosion rate was 1.092 mm/y. The weight loss for lotus stem AgNPs in iron coupon 24.4 mg and corrosion rate was 0.141 mm/y, mild steel coupon 10.2 mg and corrosion rate was 0.589 mm/y. The weight loss for lotus flower AgNPs in iron coupon 0.39 mg and corrosion rate was 0.002 mm/y, mild steel coupon 0.19 mg and corrosion rate was 0.001 mm/y (Fig. 9). It indicates that the corrosion rate was lower in the presence of AgNPs, when compared to bacterial AgNPs which is due to the adsorption of bacteria with the organic complex AgNPs acts as a good inhibitor for anticorrosion. The reduction of oxygen by bacteria in the electrolyte is also one of the reasons for the low corrosion rate (Maruthamuthu *et al*. 2011).

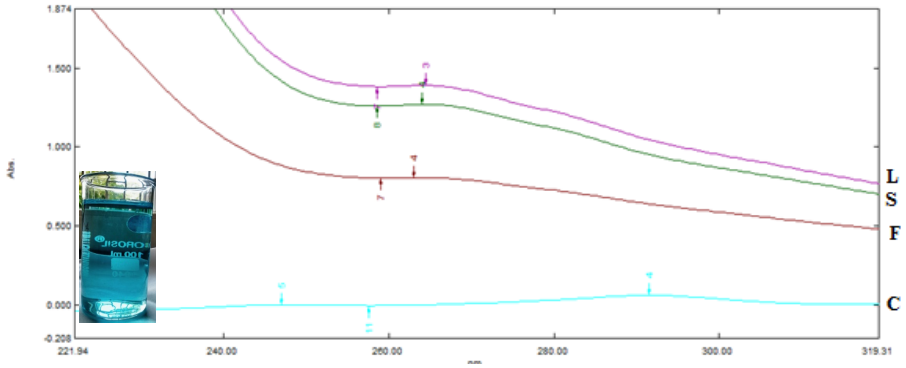

(a) Initial (12:00) Control-Methylene blue dye, AgNPs (Leaf, stem and Flower extracts) + Dye

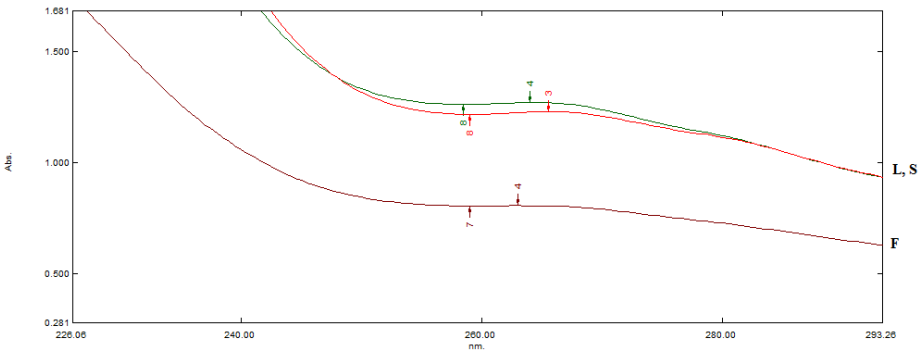

(b) 1:00

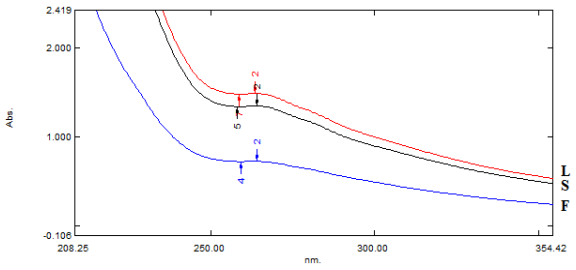

(c) 2:00

Fig. 10 Photo-catalytic degradation of methylene blue using *Nelumbo nucifera* silver nanoparticles (leaf, stem and flower) extracts at different time intervals

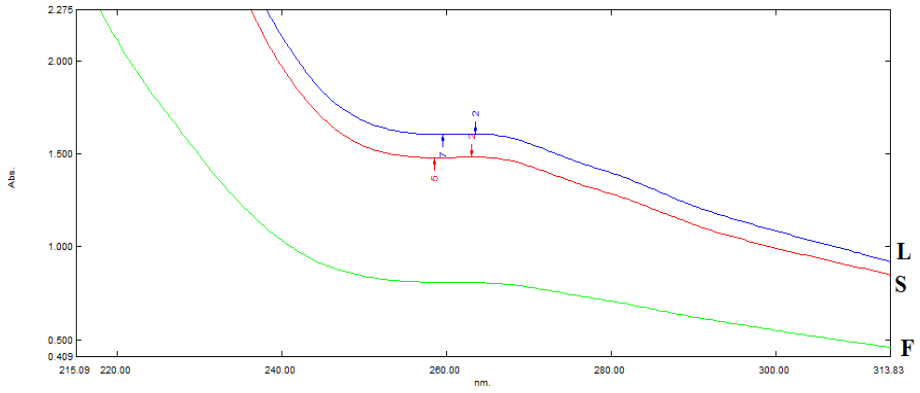

(d) 3:00

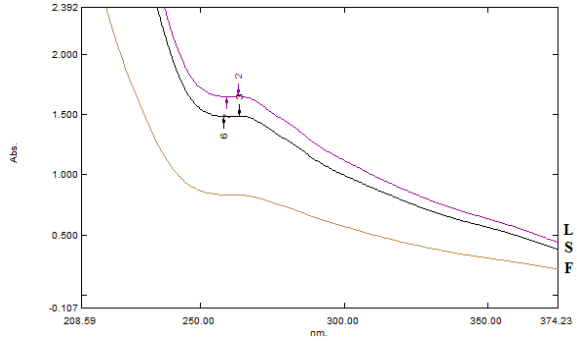

(e) 4:00

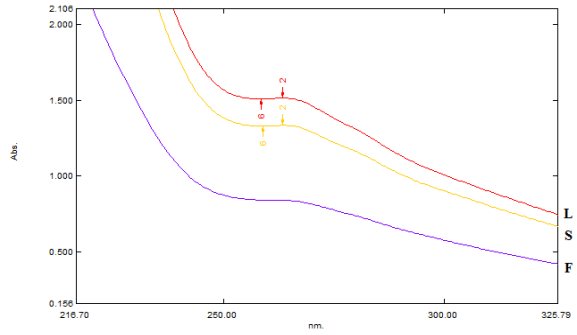

(f) 5:00

Fig. 10 Continued

3.8 Photo-catalytic degradation of dye

Photo-catalytic degradation of methylene blue dye was investigated using biosynthesized silver nanoparticles by *Nelumbo nucifera* (leaf, stem and flower) solar irradiation technique at different time intervals as shown in (Figs. 10(a), (b), and (c)). The characteristic absorption peak of methylene blue solution was found to be 290 nm. Degradation of methylene blue was visualized by increase in peak intensity within 5 h of incubation time. There is no considerable shift in peak

position for methylene blue solution without exposure to Ag nano-catalysts (Control). Solar light was found to be faster in decolorizing methylene blue solution in the presence of silver nanoparticles, silver acts as a metal catalyst. Here when compared to *Nelumbo nucifera* leaf, stem silver nanoparticles *Nelumbo nucifera* flower mediated synthesized silver nanoparticles shown effective degradation of dye. The adsorption of Ag nanoparticles on the methylene blue solution was initially low and further increased with constant increase in time and the percentage of dye degradation. Altogether, the photo-catalytic properties of Ag nanoparticles in visible light may be well due to excitation of Surface Plasmon Resonance, In general, the greater the amount of the photo-catalyst, the higher the rate of reaction due to increased active sites of the photo-catalyst would be. However, at the same time more photo-catalyst would also have induced greater aggregation, which resulted in the decrease in the surface area of the photo-catalyst, making a significant fraction of the catalyst to be inaccessible to adsorbing the dye (Vanaja *et al*. 2014).

4. Conclusions

The synthesis of silver nanoparticles through bio-reduction of silver nitrate using aqueous leaf, stem and flower extracts of N. nucifera was demonstrated. FT-IR results suggest that proteins present in the extract were largely responsible for the bio-reduction of the silver nitrate into silver nanoparticles. The weight loss indicates that the corrosion rate was higher in presence of bacteria when compared to the control. The photo-catalytic activity was observed in the system using a combination of oxidant and photo-catalyst irradiation under UV light. The present study, it is found that the use of Nelumbo nucifera extracts (Leaf, Stem and Flower) for synthesis of silver nanoparticles exhibits excellent antimicrobial activity can be used in biofilms degradation in water distribution systems, anticorrosion activity can be used in prevention of corrosion formation by applying coatings and Photo-catalytic dye degradation activity against methylene blue dye molecules and can be used in water purification systems and for dye production industries.

Acknowledgments

Authors are thankful to Acharya N.G. Ranga Agricultural University for providing research facility at institute of Frontier Technology, Regional Agricultural Research Station, Tirupati to carry out this part of the research work.

References

Abdel-Aziz, M.S., Shaheen, M.S., El-Nekeety, A.A. and Abdel-Wahhab, M.A. (2014), "Antioxidant and antibacterial activity of silver nanoparticles biosynthesized using Chenopodium murale leaf extract", *J. Saudi Chem. Soc*., **18**(4), 356-363.

Alarcon, E.I., Udekwu, K., Skog, M., Pacioni, N.L., Stamplecoskie, K.G., González-Béjar, M., Polisetti, N., Wickham, A., Richter-Dahlfors, A., Griffith, M. and Scaiano, J.C. (2012), "The biocompatibility and antibacterial properties of collagen-stabilized, photochemically prepared silver nanoparticles", *Biomater*., **33**(19), 4947-4956.

Aneja, K.R. (2003), *Experiments in Microbiology Plant Pathology Tissue Culture and Mushroom Production Technology*, (3rd Edition), New Age International Publisher, India.

Bo, L., Yang, W., Chen, M., Gao, J. and Xue, Q. (2009), "A simple and 'green' synthesis of polymer-based

silver colloids and their antibacterial properties", *Chem. Biodivers.*, **6**(1), 111-116.
Brindha, D. and Arthi, D. (2010), "Antiplatelet activity of white and pink *Nelumbo nucifera* Gaertn flowers", *Brazil. J. Pharm. Sci.*, **46**(3), 579-583.
Duke, J.A., Bogenschutz-Godwin, M.J., du Cellier, J. and Duke, A.K. (2002), *Handbook of Medicinal Herbs*.
Guidelli, E.J., Ramos, A.P., Zaniquelli, M.E.D. and Baffa, O. (2011), "Green synthesis of colloidal silver nanoparticles using natural rubber latex extracted from Hevea brasiliensis", *Acta Part A*, **82**(1), 140-145.
Hirsch, T., Zharnikov, M., Shaporenko, A., Stahl, J., Weiss, D. and Wolfbeis, O.S. (2005), "Size controlled electrochemical synthesis of metal nanoparticles on monomolecular templates", *Angew. Chem. Int. Ed.*, **44**(41), 6775-6778.
Kouvaris, P., Delimitis, A., Zaspalis, V., Papadopoulos, D., Tsipas, S.A. and Michailidis, N. (2012), "Green synthesis and characterization of silver nanoparticles produced using Arbutus Unedo leaf extract", *Mater. Lett.*, **76**, 18-20.
Maruthamuthu, S., Nagendran1, T., Anandkumar, B., Karthikeyan, M.S., Palaniswamy, N. and Narayanan, G. (2011), "Microbiologically influenced corrosion on rails current science", **100**(6), 870-880.
Mukherjee, P.K., Mukherjee, D., Maji, A.K., Rai, S. and Heinrich, M. (2009), "The sacred lotus (*Nelumbo nucifera*)-phytochemical and therapeutic profile", *J. Pharm. Pharmacol.*, **61**(4), 407-422.
Padil, V.V.T. and Cernik, M. (2013), "Green synthesis of copper oxide nanoparticles using gum karaya as a biotemplate and their antibacterial application", *Int. J. Nanomed.*, **8**, 889-898.
Panacek, A.L., Kivtek, L., Prucek, R., Milan, K., Vecerovam R, and Pizurova, N. (2006), "Silver colloid nanoparticles: synthesis, characterization, and their antibacterial activity", *J. Phys. Chem. B*, **110**(33), 16248-16253.
Panacek, A., Kolar, M., Vecerova, R., Prucek, R., Soukupova, J., Krystof, V., Hamal, P., Zboril, R. and Kvıtek, L. (2009), "Antifungal activity of silver nanoparticles against Candida spp.", *Biomaterials*, **30**(31), 6333-6340.
Prabha, S., Supraja, N., Garud, M. and Prasad, T.N.V.K.V. (2014), "Synthesis, characterization and antimicrobial activity of Alstonia scholaris bark-extract-mediated silver nanoparticles", *J. Nanostruct. Chem.*, **4**(4), 161-170. DOI: 10.1007/s40097-014-0132-z
Prabhu, D., Arulvasu, C., Babu, G., Manikandan, R. and Srinivasan, P. (2013), "Biologically synthesized green silver nanoparticles from leaf extract of Vitexnegundo L. induce growth-inhibitory effect on human colon cancer cell line HCT15 Process", *Biochemistry*, **48**(2), 317-324.
Prasad, T.N.V.K.V., Kambala, V.S.R. and Naidu, R. (2011), "A critical review on biogenic silver nanoparticles and their antimicrobial activity", *Curr. Nanosci.*, **7**(4), 531-544.
Prucek, R., Tucek, J., Kilianova, M., Panacek, A., Kvıtek, L., Filip, J., Kolar, M., Tomankova, K. and Zboril, R. (2011), "The targeted antibacterial and antifungal properties of magnetic nanocomposite of iron oxide and silver nanoparticles", *Biomaterials*, **32**(21), 4704-4713.
Rastogi, L. and Arunachalam, J. (2011), "Sunlight based irradiation strategy for rapid green synthesis of highly stable silver nanoparticles using aqueous garlic (Allium sativum) extract and their antibacterial potential", *Mater. Chem. Phys.*, **129**(1), 558-563.
Salem, W.M., Haridy, M., Sayed, W.F. and Hassan, N.H. (2014), "Antibacterial activity of silver nanoparticles synthesized from latex and leaf extract of Ficus sycomorus", *Ind. Crops. Prod.*, **62**, 228-234.
Shanmugam, N., Rajkamal, P., Cholan, S., Kannadasan, N., Sathishkumar, K., Viruthagiri, G. an Sundaramanickam, A. (2014), "Biosynthesis of silver nanoparticles from the marine seaweed Sargassum wightii and their antibacterial activity against some human pathogens", *Appl. Nanosci.*, **4**(7), 881-888. DOI: 10.1007/s13204-013-0271-4
Shen, M.J., Schopf, J.W., Harbottle, G., Cao, R.J., Ouyang, S., Zhou, K.S., Southon, J.R. and Liu, G.H. (2002), "Long-living lotus: Germination and soil-irradiation of centuries-old fruits, and cultivation, growth, and phenotypic abnormalities of offspring", *Am. J. Botany*, **89**(2), 236-247.
Shen-Miller, J., Mudgett, M.B., Schopf, J.W., Clarke, S. and Berger, R. (1995), "Exceptional seed longevity and robust growth: Ancient sacred lotus from China", *Am. J. Botany*, **82**(11), 1367-1380.
Sivakumar, P., NethraDevi, C. and Renganathan, S. (2012), "Synthesis of silver nano particles using Lantana camara fruit extract and its effect on pathogens", *Asian J. Pharm. Clin. Res.*, **5**(3), 97-101.

Sreekanth, T.V.M., Nagajyothi, P.C., Supraja, N. and Prasad, T.N.V.K.V. (2014), "Evaluation of the antimicrobial activity and cytotoxicity of phytogenic gold nanoparticles", *Appl. Nanosci.*, **5**(5), 595-602. DOI: 10.1007/s13204-014-0354-x

Sri Sindhura, K., Prasad, T.N.V.K.V., Panner Selvam, P. and Hussain, O.M. (2013), "Synthesis and characterization of phytogenic zinc nanoparticles and their antimicrobial activity", *Appl. Nanosci.*, **4**(7), 819-827.
DOI: 10.1007/s13204-013-0263-4

Sulaiman, G.M., Mohammed, W.H., Marzoog, T.R., Al-Amiery, A.A.A., Kadhum, A.A.H. and Mohamad, A.B. (2013), "Green synthesis, antimicrobial and cytotoxic effects of silver nanoparticles using Eucalyptus chapmaniana leaves extract", *Asian Pac. J. Trop. Biomed.*, **3**(1), 58-63.

Supraja, N., Prasad, T.N.V.K.V., Giridhara Krishna, T. and David, E. (2016), "Synthesis, characterization, and evaluation of the antimicrobial efficacy of Boswellia ovalifoliolata stem bark-extract-mediated zinc oxide nanoparticles", *Appl. Nanosci.*, **6**(4), 581-590. DOI: 10.1007/s13204-015-0472-0

Tomsic, B., Simoncic, B., Orel, B., Cerne, L., Tavcer, P., Zorko, M. and Jerman, A. (2008), "Sol–gel coating of cellulose fibers with antimicrobial and repellent properties", *Sol-Gel Sci. Technol.*, **47**(1), 44-57.

Vanaja, M., Paulkumar, K., Baburaja, M., Rajeshkumar, S., Gnanajobitha, G., Malarkodi. C., Sivakavinesan, M. and Annadurai, G. (2014), "Degradation of methylene blue using biologically synthesized silver nanoparticles", *Bioinorg. Chem. Appl.*, **2014**, Article ID 742346.

Vijayakumar, R., Devi, V., Adavallan, K. and Saranya, D. (2011), "Green synthesis and characterization of gold nanoparticles using extract of anti-tumor potent Crocus sativus", *Phys. E*, **44**(3), 665-671.

Yilmaz, M., Turkdemir, H., Akif Kilic, M., Bayram, E., Cicek, A., Mete, A. and Ulug, B. (2011), "Biosynthesis of silver nanoparticles using leaves of Stevia rebaudiana", *Mater. Chem. Phys.*, **130**(3), 1195-1202.

Yoon, C.K. (1996), *Heat of Lotus Attracts Insects and Scientists*, New York Times.

Yoon, J.S., Kim, H.M., Yadunandam, A.K., Kim, N.H., Jung, H.A., Choi, J.S., Kim, C.Y. and Kim, G.D. (2013), "Neferine isolated from *Nelumbo nucifera* enhances anti-cancer activities in Hep3B cells: molecular mechanisms of cell cycle arrest, ER stress induced apoptosis and anti-angiogenic response", *Phytomed.*, **20**(11), 1013-1022.

Zhong, G., Chen, Z.D. and We, Y.M. (2007), "Physicochemical properties of lotus (*Nelumbo nucifera* Gaertn.) and kudzu (*Pueraria hirsute Matsum*.) starches", *Int. J. Food Sci. Technol.*, **42**(12), 1449-1455.